

EEG-based asynchronous BCI control of a car in 3D virtual reality environments

ZHAO QiBin¹, ZHANG LiQing^{1†} & CICHOCKI Andrzej²

¹ Department of Computer Science and Engineering, Shanghai Jiao Tong University, Shanghai 200240, China;

² Laboratory for Advanced Brain Signal Processing, RIKEN Brain Science Institute, Saitama 351-0198, Japan

Brain computer interface (BCI) aims at creating new communication channels without depending on brain's normal output channels of peripheral nerves and muscles. However, natural and sophisticated interactions manner between brain and computer still remain challenging. In this paper, we investigate how the duration of event-related desynchronization/synchronization (ERD/ERS) caused by motor imagery (MI) can be modulated and used as an additional control parameter beyond simple binary decisions. Furthermore, using the non-time-locked properties of sustained (de)synchronization, we have developed an asynchronous BCI system for driving a car in 3D virtual reality environment (VRE) based on cumulative incremental control strategy. The extensive real time experiments confirmed that our new approach is able to drive smoothly a virtual car within challenging VRE only by the MI tasks without involving any muscular activities.

BCI, EEG, ERD/ERS, CSFP, TRSD/TRSS

Real-time interfaces between the brain and electro-mechanical devices could be used to restore sensory and motor functions lost from injury or disease^[1,2]. Recent studies on invasive BCI have demonstrated that monkeys and humans are able to control external devices such as computer cursor by using brain signals^[3-9]. Noninvasive BCI has in the recent years become a highly active research topic in neuroscience, engineering, and signal processing^[10-14]. The BCI which decodes the user's intent from scalp-recorded encephalogram (EEG) activity, can be used for basic communication and control^[15-18]. The subjects has to learn the self-control of a specific EEG feature and the system automatically adapts to the specific brain signals of each user by employing advanced techniques of machine learning and signal processing^[19-23]. While BCI research hopes to create new communication channels for severely handicapped people by utilizing their brain signals, recently efforts have been focused also on developing potential applications in rehabilitation, multimedia communication, virtual reality and entertainment/relaxation^[24,25].

Unfortunately, there is a widespread belief that complex control functions, such as robotic arms or neuroprosthesis, could probably not be achieved by noninvasive methods such as EEG which sum inputs from millions of neurons, owing to their poor resolution of brain activity^[26,27]. In other words, relatively low performance of noninvasive BCI remains a major obstacle. In fact, the speed and accuracy of the most existing BCIs are still far lower than the systems relying on eye movements, no matter whether they are invasive or non-invasive. Most of the current EEG-based BCI systems have an information transfer rate (ITR) below 0.5 bps.

Our main objective was to develop a new prototype of noninvasive MI-based BCI, using EEG recorded from scalp, which can provide more complex control tasks

Received August 8, 2008; accepted October 24, 2008

doi: 10.1007/s11434-008-0547-3

†Corresponding author (email: zhang-lq@cs.sjtu.edu.cn)

Supported by the National High-Tech Research Program of China (Grant No. 2006AA01Z125) and the National Basic Research Program of China (Grant No. 2005CB724301)

(i.e., driving a car) in real time than previously reported. We exploit not only the types of MI (e.g., imaginary hands and feet movements) for determining the rotation directions of steering wheel, but also the duration of specific MI, which can be viewed as the amplitude of corresponding command, is used for controlling the sophisticated steering angle in a continuously changing manner. Therefore, the user can freely navigate a car by adjusting the steering wheel angle. Moreover, he/she can speed up or automatically slow down the car. For this purpose, we have designed a cumulative incremental control (CIC) strategy, which can continuously update the current MI duration in an incremental manner and online reflects the current strength of corresponding MI tasks. In contrast to two or three discrete commands of most existing noninvasive BCIs, our system demonstrates that elaborated and smooth control functions, such as car speed and steering wheel angle, can be achieved in real time by modulating duration time of ERD/ERS corresponding to the specific MI tasks. In fact, our BCI system uses more flexible asynchronous protocols in which the subject can make self-paced decisions any time by switching among various MI tasks.

Real-time experiments show that noninvasive BCI is able to accomplish quite complicated control tasks, such as driving a car in rapidly changing 3D VRE. Furthermore, our BCI system provides a good tradeoff between response speed and reliability by selecting an optimal length of the sliding window that produces the maximum ITR. The performance results indicate that we are able to increase the performance and robustness of noninvasive MI-based BCIs working in real time.

1 Task-related sustained desynchronization

This section provides some neurophysiological evidence suggesting a new mechanism for BCIs. It is well known that sensorimotor rhythms (SMR) decrease with movement or imagery of movement and increase in the postmovement period or during relaxation, which is referred to as event related desynchronization (ERD) or synchronization (ERS)^[28,29]. It has been shown that the human motor cortex generally exhibits transient ERD/ERS responses, which are time locked to cue stimulus. However, most previous studies were mainly focused only on the detection and latency of ERD/ERS. Moreover, it was assumed that each of such events can

only produce ERD/ERS over a short period of time, which can be detected during a fixed time interval time-locked to the cue stimulus. Therefore, most existing ERD/ERS based BCI systems detect specific mental activity in a so-called synchronous control manner.

An important question is whether subjects can produce continuous or sustained ERD/ERS, which can be viewed as steady state of MI task analogous to steady-state visual evoked potential (SSVEP) or auditory steady-state responses (ASSR). Using this conception, we designed an alternative experimental paradigm by performing the continuous and repetitive MI tasks such as grasping hands with an approximate fixed frequency. We have confirmed our hypothesis that the ERD sustains as long as the MI tasks are performed continuously and repetitively. The rationale for this alternative is that the repetitive MI tasks drive the cortical response into an oscillatory “steady state” and elicit the sustained mental state in corresponding motor area.

To provide neurophysiological evidence of the sustained ERD/ERS, we conducted experiments for four subjects (young health men aged 24–30). Our results demonstrate that three out of four subjects are capable of producing the sustained desynchronization phenomena by performing continuous and repetitive MI tasks even without any training. The results shown in Figure 1 demonstrate our hypothesis about sustained ERD/ERS phenomena which is observed throughout the whole duration of 4 s trials. This can be interpreted as follows: During repetitive hand MI, contralateral area is directly involved in the task for the whole duration of mental task, resulting in the continuous and sustained activated/deactivated state of contralateral/ipsilateral cortical area at the same time, which in turn leads to the continuous and sustained ERD/ERS in contralateral/ipsilateral motor area. We call this phenomena task related sustained desynchronization/synchronization (TRSD/TRSS) or steady state event related (de)synchronization. The TRSD/TRSS is sustained ERD/ERS associated with the MI tasks that repeat at a constant frequency and can be viewed as the superposition of successive single-trial ERD/ERS for the specific MI events.

We can conclude that ERD/ERS are responses produced by discrete short events, whereas TRSD/TRSS are produced by continuous and repetitive MI tasks. The key feature of TRSD/TRSS is that it might provide also information about MI duration. Therefore, the duration

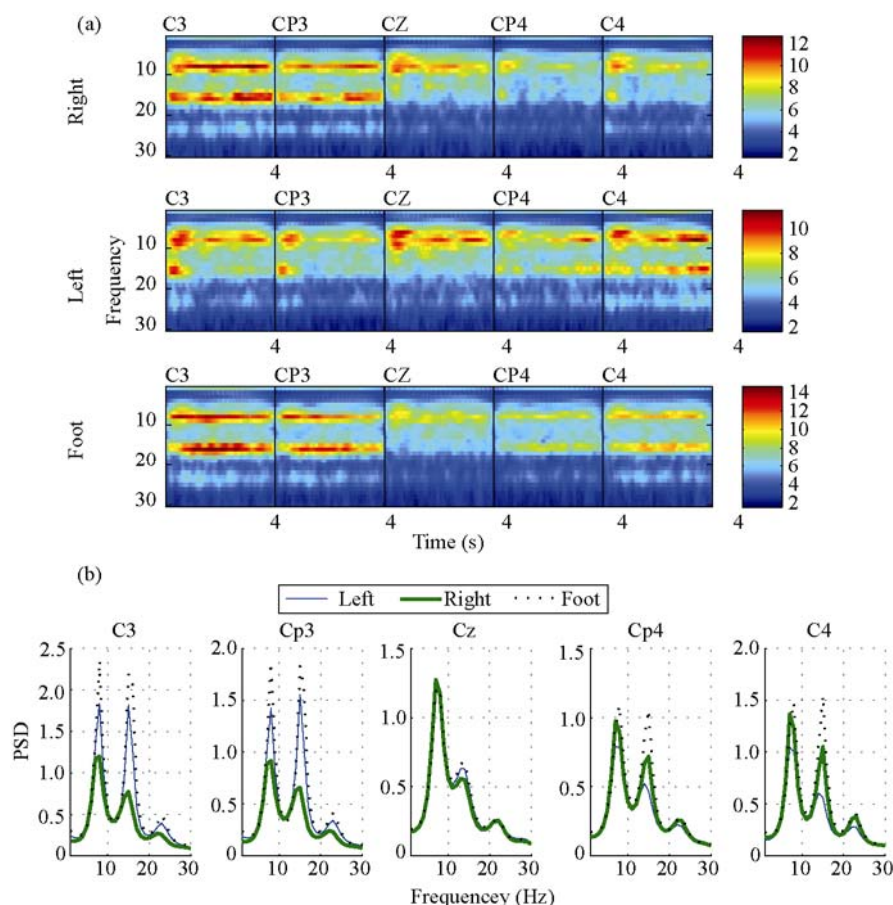


Figure 1 TRSD/TRSS phenomena. (a) Averaged time-frequency distribution of 5 channels EEG during 3 MI tasks (left hand, right hand and foot). The TRSS in C3, Cp3 and TRSD in C4, Cp4 for subject-specific frequency band are obviously seen during left hand MI (first row) whereas similar phenomena with opposite hemisphere area during right hand MI are displayed in the second row. During left foot MI (third row), TRSD in Cz is clearly seen. Meanwhile, C4 and Cp4 also have TRSD to some degree. (b) Averaged power spectrums in 5 channels which indicate the difference of power distribution in each channel during three MI tasks.

of TRSD/TRSS provides a new dimension for controlling external devices by generating an additional control parameter that is a continuous variable. In contrast to two or three discrete commands that are typically used in most existing BCI, the duration of TRSD/TRSS, which has been recognized as the magnitude of specific control command, can be modulated to provide more sophisticated control functions. Furthermore, ERD/ERS are non-phase-locked but time-locked to cue stimulus whereas TRSD/TRSS are non-phase-locked and non-time-locked. Thus, the transition between various types MI can be detected continuously by detecting the transition of TRSD/TRSS patterns. Therefore, TRSD/TRSS are more suitable for asynchronous BCI system.

2 Mind-driven car in 3D virtual reality environment

The task of our asynchronous BCI system, called

“Mind-Driven Car”, is to drive a virtual car in 3D dynamically changing VRE without any external cue stimulus. In order to test whether the subjects are able to freely control the orientation and speed of virtual car running along the narrow road in VRE, two virtual scenarios with different road curves are designed for evaluation of subjects’ driving performance:

(i) A straight road with several traffic cones arranged in central line was presented and the distance between every two adjacent traffic cones was equal. The task in this scenario was to drive the car bypassing each traffic cone along a special S-shaped pathway (Figure 2(a)).

(ii) The looped curve road with several rapid left and right turns was presented (Figure 2(b)). The task in this scenario was to drive the car along the curve road and try to keep the car running on the road with possibly maximal speed.

The evaluation criteria for both the scenarios were

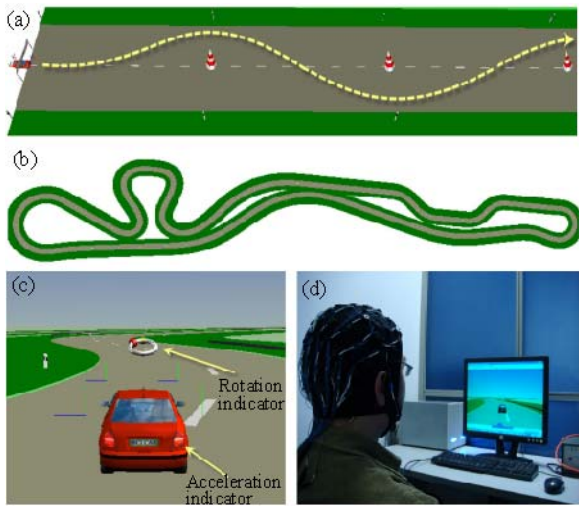


Figure 2 Experimental design. (a) Scenarios I with the straight road. The subjects are instructed to drive the car along the S shape pathway just like the yellow line in the figure. (b) The pathway of the curve road in scenarios II. (c) Screen shot of virtual reality environment and virtual car. The two marked indicator represent the feedback for subjects. The steering wheel indicates the steering angle and the taillight indicates the state (on/off) of the accelerator. (d) Picture of a subject during the experiment.

similar. A subject was considered to fail whenever the running car touched the road border. Moreover, the best subject should hold the car in a possibly high speed so that he can finish one run in a shortest time.

In order to transform thought modulated EEG signals into an output signal that controls virtual car within VRE and to make the car run smoothly, the output commands of the classifier were used to control the angle of steering wheel and accelerator (i.e., gas pedal) rather than directly control orientation and position of the car in VRE. Furthermore, to make a best turn within each scenario, the steering wheel must be rotated to a suitable angle and returned in time, otherwise we may suffer a risk of running out of the road. Due to the non-stationarity of EEG signals, incorrect classifications are unavoidable, which makes it more difficult to drive the car (e.g., oscillatory incorrect classification may result in fluctuation between left turn and right turn). Therefore, in contrast to the crude control with two or three discrete commands for most current BCI, the big challenges for our system are how to provide accurate and robust control of steering angle and to maximally avoid the influence of incorrect classification.

To realize successful drive strategy, it is necessary to detect three MI states (i.e., left hand, right hand and foot). It is worth noting that we use statistical rejection criteria that help to address an important aspect of a BCI,

namely “relaxation” state where the user is not involved in any particular mental task. Whenever the classifier cannot recognize MI states with confidence above specific threshold (typically 90%), our BCI system consider them as relaxation state. Therefore, the four MI states of left, right, foot and relaxation are decoded and projected to four control commands of turning left (L) or right (R), speedup (S) and no command (NC) respectively.

During the online process, the car position and orientation were updated continuously every 0.05 s according to current steering angle (i.e., turning angular speed) and accelerator state. Meanwhile, the steering wheel and taillight state (indicating speed up or speed down) of a virtual car were used as feedback presented continuously (Figure 2(c)), which represented the current running state impacted by output command of classifier. In order to provide fast detection of MI state transition, the predefined sliding time window was used for feature extraction and classification, and output commands were updated every 0.125 s. By this strategy, the subjects can freely determine which MI task to perform at arbitrary time. Figure 2(d) shows a screen shot of experiment process.

3 Methods

3.1 Common spatial frequency patterns (CSFP)

The common spatial patterns (CSP) algorithm is a highly successful method for efficiently calculating spatial patterns for classification of brain signals^[30–32]. However, the performance will suffer from a non-discriminative brain rhythm which has an overlapping frequency range with most discriminative brain rhythm. On the other hand, the frequency band on which the CSP algorithm operates is either selected manually or unspecifically set to a broad band filter, which is likely to deteriorate the performance by using inappropriate frequency band. In this paper, we propose a new algorithm of common spatial frequency patterns (CSFP) which allows for the simultaneous optimization of spatial and frequency patterns enhancing discriminability of EEG signals with a small number of channels. Hence the performance outperforms CSP on average, and in cases where the frequency ranges of most discriminative rhythm for each class are different, a considerable improvement of classification accuracy can be achieved.

To accommodate non-stationarity frequency analysis, continuous wavelet transform can enable us to obtain an improved tradeoff between temporal resolution and frequency resolution through varying the window length over frequencies. The continuous wavelet transform (CWT) of the EEG signal $x^{c,k}(\tau)$ is defined as

$$W^{c,k}(a,t) = \frac{1}{\sqrt{a}} \int_{-\infty}^{+\infty} x^{c,k}(\tau) \psi\left(\frac{\tau-t}{a}\right) d\tau, \quad (1)$$

where t denotes the time shift, a denotes the scale and ψ is the wavelet function, and $W^{c,k}(a,t)$ represents the CWT of the data segment $x^{c,k}(\tau)$, c represents channel index and k represents EEG trial number. Although many types of wavelets are available, Morlet wavelets seem to be appropriate for time-frequency analysis of EEG signals. Since the scale parameter a is related to frequency f by the relation $a = \omega_0/(2\pi f)$, we finally obtain a simple formula

$$\hat{W}^{c,k}(f,t) = W^{c,k}\left(\frac{F_c}{fT}, t\right), \quad (2)$$

where $\hat{W}^{c,k}(f,t)$ denotes the time-frequency coefficient at channel c , frequency f and time t of k -th trial EEG signals given by $x^{c,k}(\tau)$; F_c is the central frequency of the wavelet function in Hz; T is the sampling period of the signal. Thus time-frequency distributions (TFD) are constructed by setting f from the lowest to the highest frequency, which is of interest. We define

$$P_k^{c,f} = \hat{W}^{c,k}(f,t). \quad (3)$$

Then we can form a time-frequency distribution matrix for each channel and a spatio-temporal distribution matrix for each frequency bin, i.e.,

$$U_k^c = \left(P_k^{c,f_1}, P_k^{c,f_2}, \dots, P_k^{c,f_m} \right)^T \quad (4)$$

and

$$V_n^f = \left(P_k^{c_1,f}, P_k^{c_2,f}, \dots, P_k^{c_n,f} \right)^T. \quad (5)$$

U_k^c denotes time-frequency matrix for k -th EEG trial at channel c , in which the frequency varies in the range from f_1 to f_m and V_k^f denotes spatio-temporal matrix for k -th EEG trial at frequency f , in which the channel varies in the range from c_1 to c_n . In order to reconstruct the entire time-frequency distribution of the EEG signal, we append the U_k^c of all channels or V_k^c of all frequency bins, i.e.,

$$Y_k = \begin{pmatrix} U_k^{c_1} \\ U_k^{c_2} \\ \vdots \\ U_k^{c_n} \end{pmatrix} \text{ or } Y_k = \begin{pmatrix} V_k^{f_1} \\ V_k^{f_2} \\ \vdots \\ V_k^{f_m} \end{pmatrix}. \quad (6)$$

Using this notation, the class-covariance matrices are given as

$$\Gamma_i = \sum_{k \in \text{class}_i} \frac{Y_k Y_k^T}{\text{tr}(Y_k Y_k^T)}, \quad (7)$$

where $Y_k \in R^{N \times M}$ denotes a time-frequency matrix of the k -th trial EEG, N is the number of channels number \times frequency number (i.e., $n \times m$), M is the number of samples in each trial, and class _{i} refers to the i -th class of the training data.

Then the optimization objective of CSFP is to find maximal discriminative spatial and frequency combination patterns described by W . The vector $W_k \in R^d$ ($d = n \times m$), which refers to the p -th column of W , maximizes the variance in one class while simultaneously minimizes the total variance in the whole class. Each vector W is therefore found by solving the following optimisation problem:

$$\arg \max_w \frac{W^T S_I W}{W^T S_T W}. \quad (8)$$

In order to find the maximum discriminative patterns for each class, we can set the two matrices S_I and S_T as follows:

$$S_I = \Gamma_i \Big|_{i=1}^M, \quad S_T = \frac{1}{M} \sum_{i=1}^M (\Gamma_i), \quad (9)$$

where S_I is class-specific covariance matrix of TFD in eq. (7) and S_T is total covariance matrix of M class data. By optimizing the criteria in eq.(8), we can get projection matrix $W^{(i)}$ i.e., spatial frequency patterns, for each class i . The number of projection vector in each $W^{(i)}$ can be selected by cross validation on training data. Finally, the $W^{(i)} \Big|_{i=1}^M$ are combined into one matrix $W_{csfp} = [W^{(1)}, W^{(2)}, \dots, W^{(M)}]$ which can be seen as maximal discriminative spatial frequency patters for multi-class EEG signals.

With the projection matrix, the TFD Y_k of EEG signals can be projected onto W_{csfp} as

$$Z_k = W_{csfp}^T Y_k. \quad (10)$$

Therefore, Z_k denotes the maximal discriminative components for multi-classes data, which are obtained

by optimizing the spatial and frequency patterns simultaneously.

Finally, the features used for the classification are obtained by projecting the TFD of EEG data according to Eq.(10). Typically one would retain only a small number of l projections vectors, which contain most of the discriminative information for each class. These projections are given by the columns of W_{csfp} corresponding to the l largest eigenvalues for each of M classes. Based on the projected signal trials Z_k^p , $p = 1, \dots, M \times 1$, a classifier is trained on the the feature vectors obtained by normalizing and log-transforming the variances of projected EEG series as

$$f_k = \log \left(\frac{\text{diag}(Z_k Z_k^T)}{\text{tr}(Z_k Z_k^T)} \right), \quad (11)$$

where $f_k \in R^{M \times l}$ are projected CSFP features vector of k -th EEG trial. The log transformation serves to approximate normal distribution of the data.

However, the feature vector f_k only considered the relative power distribution between each CSFP component. The experiment results demonstrated that the total power of all CSFP components are also important for discrimination of different MI tasks, especially between the hand and foot MI. To further improve the classification performance, we constructed another part of feature vector defined as

$$d_k^j = \left| \sum_{i=1}^{M \times l} \text{var}(Z_k^i) - \frac{1}{N_j} \sum_{k \in \text{class}_j} \left(\sum_{i=1}^{M \times l} \text{var}(Z_k^i) \right) \right|, \quad (12)$$

where j denotes the classes index from 1 to M . The N_j is the number of trials belonging to j -th class, whereas, the d_k^j denotes the distance between total power of all CSFP components and averaged power of j -th class. Via normalization by $d_k^j / \|d_k^j\|^2$, we obtained the feature vector of k -th trial that reflected the relative distance distribution to each class. Finally, we combined these two parts into one feature vector, i.e., $[f^T, d^T]^T$, which was then used to train the classifier. Specifically we applied a linear support vector machine (SVM) as classifier, and used a 10×10-fold cross-validation to select the optimal parameters for training the classifier.

3.2 Cumulative incremental control strategy

It should be noted that, only 4 discrete commands are not enough to provide elaborated control of steering

angle and speed. Therefore, we use the duration of specific MI tasks as an additional control parameter, which can not only add more sophisticated control functions but also can prevent rapid fluctuation of car orientation caused by incorrect classifications from time to time.

For steering angle control, the classification of left/right hand MI determines specific rotating directions and the duration of specific TRSD, i.e., duration of corresponding MI task, determines the detailed steering angle. Longer duration caused larger steering angle, which alters the output commands of BCI from discrete variable to continuous variable. The steering angle is controlled by a linear equation of duration sustained time for current control command defined as

$$\theta_t = (D_t^L - D_t^R) \Delta \theta, \quad (13)$$

where D_t^L and D_t^R represents the duration for left and right commands at time t , i.e., how many previous control commands are all equal to current command. The $\Delta \theta$ is the constant angular speed which can be adjusted in subject adaptation stage to optimize the translation of subject-specific EEG into control commands, and θ_t is the steering angle at time t in which the positive and negative values denotes the rotation towards left and right respectively.

For speed control, whenever TRSD state of foot are detected, the accelerator will be turned on and increase the car speed gradually; on the contrary, when this state disappears or it is not detected, the accelerator will be turned off immediately and decrease the car speed gradually. The previous car speed v_{t-1} and specific increase or decrease are added to give the current speed of v_t . The iterative equation are expressed as

$$v_t = v_{t-1} + \delta_t^S (\Delta v_+ + \Delta v_-) - \Delta v_-, \quad (14)$$

δ_t^S is the delta function, which is equal to zero, but it will be equal to one whenever the control command is speedup (S). The Δv_+ represents the constant acceleration and Δv_- represents the negative acceleration, and meanwhile $\Delta v_+ > \Delta v_-$ are typically satisfied. This control mechanism can be interpreted as follows: once the control command of S is outputted, the car speed will be increased by Δv_+ once, otherwise, the car speed will be decreased by Δv_- once, as with the case of the gas pedal of a real car.

This can be interpreted as follows: the duration of

specific MI task has been used additionally to provide more sophisticated control, which can be called “time exchange complexity”. Furthermore, the NC state was used to reset the steering angle at zero and turn off the accelerator, which results in running forward with a deceleration of speed. According to this strategy, the incorrect classification results that usually does not have long duration will not largely impact the steering angle. This can be defined as the error tolerance ability. Hence our BCI system is more robust than most existing BCI systems.

In order to detect the duration online, we developed a new control strategy of cumulative incremental control (CIC) based on overlapped sliding window technique. At each time, the duration of specific MI is updated online according to both the current and previously generated commands. Thus, the amplitude of an actual output command is cumulated in an incremental manner and steering is rotated incrementally by a fixed angle at each step depending on whether consecutive and same MI state are detected or not. The amplitude of output command is reset at zero and steering is returned whenever the current command is different from previous commands. In other words, to drastically rotate the steering wheel, subjects need to sustain the left or right MI task for a longer duration. To drastically increase the speed, subjects need to perform the foot MI task for a longer duration. Hence, the steering angle θ_t is varied continuously within the range of $[-\pi/2, \pi/2]$ and the speed is varied continuously within the range of $[v_{min}, v_{max}]$. We have developed such a strategy because it works in a natural manner and is quite similar to real control of a car by a driver’s limbs.

3.3 Virtual reality environment

Finally, the orientation and position of the car in 3D VRE are updated every 0.05 s according to

$$\mathbf{o}_t = \mathbf{R}_{c\theta_t} \mathbf{o}_{t-1} \quad \text{and} \quad \mathbf{P}_t = \mathbf{P}_{t-1} + \mathbf{o}_t v_t, \quad (15)$$

where \mathbf{o}_t denotes the 3D orientation vector at time t whose norm is always equal to one and $\mathbf{R}_{c\theta_t}$ denotes the rotation matrix corresponding to the angle of $c\theta_t$ in which c is the fixed scale parameters between the steering wheel and car. This demonstrates that the orientation is determined by previous orientation and current rotation angle of θ_t in eq. (13). The vector \mathbf{P}_t denotes the 3D position vector in VRE at time t , which are updated according to the previous position \mathbf{P}_{t-1} ,

current orientation \mathbf{o}_t and current speed v_t in eq. (14).

4 Real time experimental results

Four healthy male subjects (ages 24–30) participated in this study. They served as volunteers and were given a complete and accurate description of the purpose, procedures, risks and benefits of participation. EEG signals with only 5 electrodes (i.e., C3, Cp3, Cz, Cp4 and C4) over the motor cortex were recorded from the scalp at a sampling rate of 250 Hz.

In the training stage, the system training and subjects’ self-adaptation were two important parts for improving the system performance. Each training run consists of 30 trials and lasts only for 3 min. To provide continuous classification of MI and detection of switching between various MI tasks, the training samples were extracted from each trial using overlapped sliding window with 0.125 s interval. One important question was how to determine the optimal length of sliding window, which is the tradeoff between accuracy and response speed. The experimental EEG data was analyzed using sliding window techniques with a window length ranging from 0.5 to 4 s. As the analyzing window length increased, the classification accuracy was greatly improved but a lower response speed of the BCI resulted. In this study, training sessions were used to select optimal subject-specific window length by which the online performance is better than 75% (lowest requirement for driving a car safely) with possibly highest ITR.

The performance of each subject was gradually improved over the training runs due to the mutually adaptive updating of the system model and self-adaptation of a human brain. Our BCI experiments show that for 3 out of 4 subjects, a classification performance above 75% can be achieved only after several training runs, while only one subject had a performance lower than 70% and he was incapable of improving performance after a few runs. Furthermore, the performance of two subjects (S1, S2) was excellent, although variability in the classification results among individuals runs occurred. The online classification accuracy of two subjects reached 91% for 4 s MI time, and even 76% for 1 s MI time. The average ITR of 0.55 bps was achieved with 1 s time window by subject S2. Surprisingly, the best performance of 70% with a very short time of 0.5 s was obtained during some runs and ITR reached 0.8 bps. We observed a significant

deterioration of performance for the MI time shorter than 0.5 s. In subject adaptation stage, we found that subjects S1 and S2 could change output commands quickly even within 0.5 s, and the maximum sustained time for specific MI states was 4 and 6 s respectively.

During experiments of driving a car in VRE, two subjects (S1, S2) were able to drive the car successfully

along predefined pathway in both scenarios. For further illustration of results, Figure 3(a) shows output commands sequence of one run with scenarios I. The real-time changes of speed and steering angle are presented in Figure 3(b) and (c), which demonstrate that speed and steering angle are controlled by both the type and duration of MI. The longer the duration to perform a

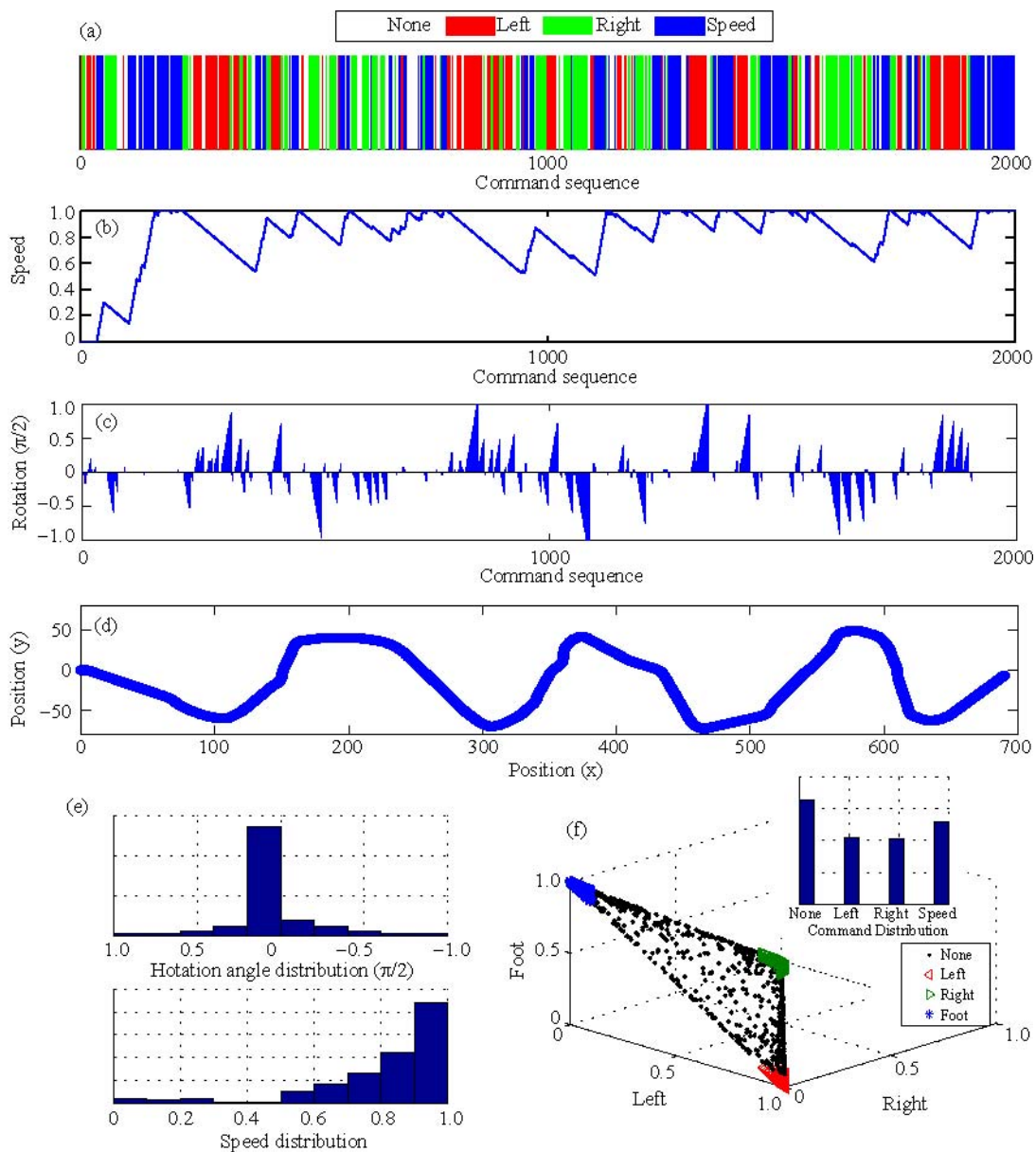


Figure 3 Real time experiment result. (a) Commands sequence (i.e., real-time classification output of MI tasks) for driving a car during 2 min. To operate the BCI, left hand (L), right hand (R) and foot (F) MI tasks are projected to left, right and speedup commands respectively. Also the NC (none) was detected. (b) Real-time changes of the car speed. Each point corresponds to the speed changed by each output command in (A). (c) Real-time steering angles corresponding to each output command. The range of steering angle is $[-\pi/2, \pi/2]$ in which the positive value represents the rotation to left whereas negative value represents the rotation to right. The large steering angle is elicited by the long duration of MI. (d) The pathway of the car running in 3D VRE. (e) The frequency of occurrence for steering angles and speed. (f) The distribution of probability (confidence) corresponding to each task. Each point represents one real-time classification result which contains three probabilities corresponding to each MI task. The output command is the one whose probability reach the threshold (red, green and blue areas), otherwise the none command is elicited (black area).

fixed MI task, the larger the steering angle will be generated. In addition, some incorrect classification as can be clearly seen in Figure 3(c), resulted in small angles deviations due to the short duration in contrast to the correction classification, hence the pathway of the car is scarcely changed by error classifications. The frequencies of occurrence for left and right commands are basically balanced (Figure 3(e)) due to the predefined pathway. The real pathway of running a car is presented in Figure 3(d), which further demonstrates the robustness of our BCI system.

The running distance of a car within a specific period of time can be used as advanced performance evaluation criteria for comparison of various subjects. Longer distance is due to the fact that the subject not only can control the steering angle correctly and bypass all traffic cones but also can drive the car with a high speed. In this study, subjects S1 and S2 bypassed 7 and 10 traffic cones respectively in 2 min. To further demonstrate the real time experiment processes, we also provide two short videos¹⁾.

One interesting aspect was that when subject S2 performed simultaneously left hand and left foot (LHF) or right hand and right foot (RHF) imagery rhythmic

movements, the TRSD on contralateral and TRSS on ipsilateral cortex are considerably enhanced. Hence, performance was better than using three basic MI tasks (i.e., left hand, right hand and both feet). This phenomenon is due to the fact that left/right foot elicited ERD on both central and contralateral cortical area because a larger number of neurons are involved in the activated state, and therefore the combination MI of LHF or RHF could produce stronger TRSD on contralateral area.

5 Conclusions

To sum up, we have developed a new MI-based BCI system for controlling such devices as virtual car. It can also serve as a new kind of game. Undoubtedly, many fundamental technological bottlenecks are to be broken through before this is realized to control a real car. Nevertheless, it seems reasonable to predict that a definitive demonstration of TRSD/TRSS phenomena and MD-Car application could act as a new type of BCI and trigger a progress of asynchronous BCI. We believe that, some day in the future, the paralyzed patients are able to drive a real car directly by thought.

- 1 Nicolelis M A L. Actions from thoughts. *Nature*, 2001, 409(6818): 403–407
- 2 Wolpaw J R, Birbaumer N, McFarland D J, et al. Brain-computer interfaces for communication and control. *Clin Neurophysiol*, 2002, 113(6): 767–791
- 3 Dornhege G. *Toward Brain-Computer Interfacing*. Cambridge, MA: MIT Press, 2007
- 4 Serruya M, Hatsopoulos N, Paninski L, et al. Instant neural control of a movement signal. *Nature*, 2002, 416(6877): 141–2
- 5 Wessberg J, Stambaugh C R, Kralik J D, et al. Real-time prediction of hand trajectory by ensembles of cortical neurons in primates. *Nature*, 2000, 408(6810): 361–365
- 6 Taylor D M, Tillery S I H, Schwartz A B. Direct cortical control of 3D neuroprosthetic devices. *Science*, 2002, 296(5574): 1829
- 7 Musallam S, Corneil B D, Greger B, et al. Cognitive control signals for neural prosthetics. *Science*, 2004, 305(5681): 258–262
- 8 Santhanam G, Ryu S I, Yu B M, et al. A high-performance brain-computer interface. *Nature*, 2006, 442(7099): 195–198
- 9 Chapin J K, Moxon K A, Markowitz R S, et al. Real-time control of a robot arm using simultaneously recorded neurons in the motor cortex. *Nat Neurosci*, 1999, 2: 664–670
- 10 Müller K R, Blankertz B. Toward noninvasive brain-computer interfaces. *IEEE Signal Processing Magazine*, 2006, 23(5): 125–128
- 11 Pfurtscheller G, Brunner C, Schlögl A, et al. Mu rhythm (de) syn-
- chronization and EEG single-trial classification of different motor imagery tasks. *NeuroImage*, 2006, 31(1): 153–159
- 12 Blankertz B, Dornhege G, Krauledat M, et al. The non-invasive berlin brain-computer interface: Fast acquisition of effective performance in untrained subjects. *NeuroImage*, 2007, 37(2): 539–550
- 13 Blankertz B, Tomioka R, Lemm S, et al. Optimizing spatial filters for robust EEG single-trial analysis. *Signal Processing Magazine*, 2008, *IEEE*, 25(1): 41–56
- 14 Sitaram R, Zhang H, Guan C, et al. Temporal classification of multichannel near-infrared spectroscopy signals of motor imagery for developing a brain: Computer interface. *NeuroImage*, 2007, 34(4): 1416–1427
- 15 Birbaumer N, Ghanayim N, Hinterberger T, et al. A spelling device for the paralysed. *Nature*, 1999, 398(6725): 297–8
- 16 Pfurtscheller G, Neuper C, Müller G R, et al. Graz-BCI: State of the art and clinical applications. *IEEE Transactions on Neural Systems and Rehabilitation Engineering*, 2003, 11(2): 1–4
- 17 Wolpaw J R, McFarland D J, Bizzi E. Control of a Two-dimensional movement signal by a noninvasive brain-computer interface in humans. *Proc Natl Acad Sci USA*, 2004, 101(51): 17849–17854
- 18 Wolpaw J R, McFarland D J, Vaughan T M, et al. The Wadsworth center brain-computer interface (BCI) research and development program. *IEEE Transactions on Neural Systems and Rehabilitation Engineering*, 2003, 11(2): 1–4

1) <http://bcmi.sjtu.edu.cn/~zhaoqibin/demos.html>

- 19 Muller K R, Krauledat M, Dornhege G, et al. Machine learning techniques for brain-computer interfaces. *Biomed Tech*, 2004, 49(1): 11–22
- 20 Dornhege G, Blankertz B, Krauledat M, et al. Combined optimization of spatial and temporal filters for improving brain-computer interfacing. *IEEE Trans Biomed Eng*, 2006, 53(11): 2274–2281
- 21 Blankertz B, Dornhege G, Lemm S, et al. The berlin brain-computer interface: Machine learning based detection of user specific brain states. *J Univ Comp Sci*, 2006, 12(6): 581–607
- 22 Muller K R, Anderson C W, Birch G E. Linear and nonlinear methods for brain-computer interfaces. *IEEE Transactions on Neural Systems and Rehabilitation Engineering*, 2003, 11(2): 165–169
- 23 Kamousi B, Liu Z, He B. Classification of motor imagery tasks for brain-computer interface applications by means of two equivalent dipoles analysis. *IEEE Transactions on Neural Systems and Rehabilitation Engineering*, 2005, 13(2): 166–171
- 24 Pfurtscheller G, Leeb R, Keinrath C, et al. Walking from thought. *Brain Res*, 2006, 1071(1): 145–152
- 25 Krepki R, Blankertz B, Curio G, et al. The berlin brain-computer interface (BBCI)-towards a new communication channel for online control in gaming applications. *Multimedia Tools Appl*, 2007, 33(1): 73–90
- 26 Fetz E. Real-time control of a robotic arm by neuronal ensembles. *Nat Neurosci*, 1999, 2: 583–584
- 27 Donoghue J. Connecting cortex to machines: Recent advances in brain interfaces. *Nat Neurosci*, 2002, 5(suppl): 1085–1088
- 28 Pfurtscheller G, Lopes da Silva F. Event-related EEG/MEG synchronization and desynchronization: basic principles. *Clin Neurophysiol*, 1999, 110(11): 1842–1857
- 29 Pfurtscheller G, Neuper C, Brunner C, et al. Beta rebound after different types of motor imagery in man. *Neurosci Lett*, 2005, 378(3): 156–159
- 30 Ramoser H, Muller-Gerking J, Pfurtscheller G. Optimal spatial filtering of single trial EEG during imagined handmovement. *IEEE Transact Neur Syst Rehabil Eng*, 2000, 8(4): 441–446
- 31 Müller-Gerking J, Pfurtscheller G, Flyvbjerg H. Designing optimal spatial filters for single-trial EEG classification in a movement task. *Clin Neurophysiol*, 1999, 110: 787–798
- 32 Wang Y, Zhang Z, Li Y, et al. BCI competition 2003-data set IV: An algorithm based on CSSD and FDA for classifying single-trial EEG. *IEEE Transactions on Biomedical Engineering*, 2004, 51(6): 1081–1086